Bone marrow mesenchymal stem cells combined with ultra-purified alginate gel as a regenerative therapeutic strategy after discectomy for degenerated intervertebral discs

Daisuke Ukeba[a], Hideki Sudo[a,b,*], Takeru Tsujimoto[a], Katsuro Ura[a], Katsuhisa Yamada[a,b], Norimasa Iwasaki[a]

[a] Faculty of Medicine and Graduate of Medicine, Department of Orthopedic Surgery, Hokkaido University, Sapporo, Hokkaido, Japan
[b] Faculty of Medicine and Graduate of Medicine, Department of Advanced Medicine for Spine and Spinal Cord Disorders, Hokkaido University, Sapporo, Hokkaido, Japan

ARTICLE INFO

ABSTRACT

Background: Because the regenerative ability of intervertebral discs (IVDs) is restricted, defects caused by discectomy may induce insufficient tissue repair leading to further IVD degeneration. An acellular bioresorbable biomaterial based on ultra-purified alginate (UPAL) gel was developed to fill the IVD cavity and prevent IVD degeneration. However, an acellular matrix-based strategy may have limitations, particularly in the elderly population, who exhibit low self-repair capability. Therefore, further translational studies involving product combinations, such as UPAL gel plus bone marrow-derived mesenchymal stem cells (BMSCs), are required to evaluate the regenerative effects of BMSCs embedded in UPAL gel on degenerated IVDs.
Methods: Rabbit BMSCs and nucleus pulposus cells (NPCs) were co-cultured in a three-dimensional (3D) system in UPAL gel. In addition, rabbit or human BMSCs combined with UPAL gel were implanted into IVDs following partial discectomy in rabbits with degenerated IVDs.
Findings: Gene expression of NPC markers, growth factors, and extracellular matrix was significantly increased in the NPC and BMSC 3D co-culture compared to that in each 3D mono-culture. *In vivo*, whereas UPAL gel alone suppressed IVD degeneration as compared to discectomy, the combination of BMSCs and UPAL gel exerted a more potent effect to induce IVD regeneration. Similar IVD regeneration was observed using human BMSCs.
Interpretation: These findings demonstrate the therapeutic potential of BMSCs combined with UPAL gel as a regenerative strategy following discectomy for degenerated IVDs.
Funding: Ministry of Education, Culture, Sports, Science, and Technology of Japan, Japan Agency for Medical Research and Development, and the Mochida Pharmaceutical Co., Ltd.

1. Introduction

Lumbar intervertebral disc (IVD) herniation constitutes a common cause of sciatica that can be treated by discectomy to remove IVD materials compressing the nerve root. However, discectomy fails to address the inherent probability of further IVD degeneration because the IVD exhibits poor capacity for self-repair [1]. Consequently, the potential remains for developing severe disabling lower back pain in addition to reherniation, which can necessitate additional surgery [2,3].

An innovative manoeuvre that could be applied at the time of discectomy to prevent these undesirable adverse effects would therefore improve surgical outcomes. Toward this end, advances in cell biology and tissue engineering have led to significant progress in the field of biological treatments to induce IVD regeneration [3]. among these, bone marrow-derived mesenchymal stem cell (BMSC) transplantation may represent a valid measure for the treatment of degenerated IVD disease [4]. In particular, the results of a randomized controlled trial confirmed the feasibility and safety of this approach for patients with chronic low back pain; moreover, BMSC-injected patients demonstrated a significant improvement in functional indices compared with those of the control patients [4].

For patients with IVD herniation, however, a carrier biomaterial is needed to prevent cell leakage and facilitate the differentiation and

Research in context

Evidence before this study

Discectomy to treat degenerated intervertebral discs (IVD) may offer temporary relief but may not induce tissue repair, especially in elderly patients with fewer endogenous nucleus pulposus cells (NPCs), and does not address the potential for further degeneration. Previously, we reported the use of an acellular bioresorbable ultra-purified alginate (UPAL) gel to prevent post-discectomy IVD degeneration and facilitate extracellular matrix (ECM) production following discectomy, with the potential for natural healing in young patients currently being evaluated in a first-in-human clinical trial.

Added value of this study

To address the potential issue of limited IVD regeneration in select patient populations, in the current study we demonstrated that the combination of bone-derived mesenchymal stem cells (BMSCs) with UPAL gel in vitro, and transplantation thereof in vivo following discectomy in a rabbit model, promoted endogenous NPC activation together with BMSC activation and differentiation into NPCs, together with growth factor and ECM production and enhanced IVD regeneration. Notably, similar results were obtained with either rabbit or human BMSCs.

Implications of all the available evidence

The findings reveal that implantation of BMSCs combined with gel is effective in preventing IVD degeneration. In addition, our results highlight the interplay between BMSCs and existing NPCs in achieving IVD regeneration. Thus, these findings demonstrate the additional therapeutic potential of BMSCs, localized at the IVD site by UPAL gel, as a regenerative strategy following discectomy for degenerated IVDs and support the future evaluation of this approach in a clinical setting, especially in an older population cohort.

activation of BMSCs [5]; nevertheless, no hydrogels are yet clinically available for use with discectomy-associated defects [2]. Recently, we reported the use of an acellular bioresorbable ultra-purified alginate (UPAL) gel to prevent post-discectomy IVD degeneration [2]. The originally developed UPAL gel is highly purified with decreased endotoxicity ($<1 \times 10^{-4}$ of that of commercially available laboratory alginate) and is thus considered suitable for clinical use [2]. Our strategy utilized $CaCl_2$ surface coverage for alginate gelation (approximately 5 min), which adjusts to diversely shaped IVD defects without necessitating suturing of the annulus fibrosis (AF) [2]. The UPAL gel facilitated extracellular matrix (ECM) production following discectomy, exhibiting sufficient biomechanical characteristics without material protrusion in rabbit and sheep models [2].

Previously, we suggested that viable endogenous nucleus pulposus (NP) cells migrated to discectomy sites filled with UPAL; persisting NP progenitor cells were also recruited, resulting in endogenous IVD repair [2]. Because residual NP tissue represents a possible source of reparative cells [2], the quantity of NP and the grade of degenerative changes may affect the ability of these cells to effect IVD repair [2]. For example, as the in vivo rabbit and sheep models of IVD degeneration applied in our previous study were created from healthy IVDs, which might show natural healing processes [2], we are currently conducting a first-in-human clinical trial in which the UPAL gel is implanted following discectomy in young patients in their 20s−40s [6]. However, an acellular matrix-based strategy may have

limitations in an elderly population including such conditions as combined lumbar canal stenosis (e.g., lumbar canal stenosis-complicated IVD herniation). Therefore, further in vivo translational studies of product combinations, such as UPAL gel plus BMSCs, are required to identify strategies to address the course of post-surgery IVD degeneration from its onset [2]. Accordingly, the purpose of the present study was to investigate regenerative effects of transplanting BMSCs embedded in UPAL gel on the degenerated IVDs following discectomy.

2. Materials and methods

2.1. Animal experimentation

All animal procedures were approved by the Institutional Animal Care and Use Committee at Hokkaido University (approval number: 13-0051) and performed in accordance with the approved guidelines. Male Japanese white rabbits (20 weeks old, 3·2−3·5 kg) were obtained from Sankyo Labo Service Corporation (Tokyo, Japan).

2.2. Preparation of rabbit NP cells (NPCs)

NP samples were obtained from lumbar IVDs (from L1/2 to L5/6; total 20 IVDs) from four rabbits following euthanization via intravenous pentobarbital overdose. The NPCs were isolated from the NP tissues and cultured as previously described [2,5,7,8]. Briefly, gelatinous NP tissues were separated from AF using a micro ear forceps under aseptic conditions. The tissue specimens were placed in culture medium containing Dulbecco's modified Eagle's medium (Sigma-Aldrich, St. Louis, MO, USA) supplemented with 10% foetal bovine serum (Nichirei Bioscience, Tokyo, Japan), 1% penicillin/streptomycin, and 1.25 mg/ml fungizone (Life Technologies, Waltham, MA, USA). Exogeneous growth factors were not used. The samples were resuspended in medium supplemented with 0.25% collagenase (Wako Pure Chemical Industries, Osaka, Japan) and incubated in a shaking incubator at 37 °C with 20% O_2 and 5% CO_2 for four hours for cell isolation by enzymatic digestion. The cells separated from the NP tissues were expanded in culture dishes and cultured with the medium as described above at 37 °C with 20% O_2 and 5% CO_2 in a humidified atmosphere. Medium was changed twice weekly and the NPCs were expanded to passage 2.

2.3. Preparation of rabbit allogeneic BMSCs

We used OriCell™ Rabbit Mesenchymal Stem Cells purchased from Cyagen (Santa Clara, CA, USA; catalogue number: RBXMX-01,001, lot number: 151114I31) as rabbit allogeneic BMSCs. These cells have been tested for characteristics, post-thaw viability, cell cycle, verification of undifferentiated state, and multipotent differentiation ability along the osteogenic, chondrogenic, and adipogenic lineages. The BMSCs were cultured according to the manufacturer's instructions, the medium as described above was replaced twice weekly, and the BMSCs were used at passage 2.

2.4. Preparation of UPAL gel and three-dimensional (3D) culture

In this study, we used UPAL gel (Mochida Pharmaceutical Co. Ltd., Tokyo, Japan) as an alginate scaffold for 3D culture as previously described [2]. The purification process of UPAL gel has been previously described [2]. Briefly, alginate in seaweed was extracted by converting to water-soluble sodium alginate via a clarification procedure [2]. As this alginate solution was highly viscous, this solution was diluted with a large amount of water using proprietary unpublished know-how technology [2]. Next, the extract was filtered to divide sodium alginate solution from fibrous residue [2]. An acid was added to isolate alginic acid from diluted solution based on

know-how technology that is particularly suitable to produce high-quality alginic acid [2].

We prepared 2% (w/v) UPAL solution dissolved in phosphate-buffered saline (Wako Pure Chemical Industries) and 102 mM $CaCl_2$ for gelation. Prior to the 3D culture, the BMSCs were fluorescently labeled with a final concentration of 20 μM 5,6 caboxyfluorescein diactetate succinimidyl ester (CFDA-SE; CFDA-SE Cell Proliferation Assay Kit; BIO RAD, Hercules, CA, USA) in accordance with the manufacturer's instructions [9]. Subsequently, the labeled BMSCs and unlabeled NPCs were encapsulated in the UPAL solution at ratio of 1:1 (each 1 $\times$ 10^6 cells/ml) [1,10], resulting in a final cell density of 2 $\times$ 10^6 cells/ml [9,10]. The UPAL/cell mixture was pipetted into 102 mM $CaCl_2$ through a 22 gauge needle for gelation (Supplementary Fig. 1). The gel beads were cultured with the medium as described above under hypoxia condition (5% O_2 and 5% CO_2) for seven days [10]. Additionally, NPCs and BMSCs were separately encapsulated in the UPAL solution with a cell density of 1 $\times$ 10^6 cells/ml. The cell density was set based on a previous study [11] comparing the effects using a different total cell number in each group. Following gelation, the gel beads were cultured under hypoxia condition in the same manner. The experimental groups were as follows: (a) NPC mono-culture; (b) BMSC mono-culture; and (c) NPC + BMSC co-culture.

At 0 and 7 days after culture, all gel beads were dissolved in 55 mM sodium citrate until the gels and cells were separated, as previously described [8]. In the NPC + BMSC co-culture group, the collected cells were sorted using a BD FACSAria III High speed cell sorter with Diva software version7.0 (BD Biosciences, San Jose, CA, USA) [1,12]. The cells fluorescing at 530 nm were identified as BMSCs and non-fluorescent cells were identified as NPCs, following exclusion of dead cells and debris.

2.5. RNA extraction and real-time quantitative reverse transcription-polymerase chain reaction (qRT-PCR)

The collected NPCs and BMSCs were lysed in 1 ml TRIzol® (Invitrogen, Carlsbad, CA, USA) and total RNA was extracted from the samples using the RNeasy Mini kit (Qiagen, Valencia, CA, USA). Real-time qRT-PCR analysis was performed using TaqMan® Gene Expression Assays and Custom TaqMan® Gene Expression Assays (Applied Biosystems, Waltham, MA, USA) (Supplementary Table 1). A cycle threshold (Ct) value was obtained for each sample, and the $2^{-\Delta Ct}$ method was used to calculate the relative mRNA expression of each target gene normalized to the Ct value of the housekeeping gene *GAPDH* [1].

2.6. In vivo *study in a rabbit degenerated IVD model*

A total of 48 rabbits were used for *in vivo* study. The sample size was determined for each of the two time points used here based on previous studies [2,7,8]. Of the 48 rabbits, 32 were randomly selected for qualitative analysis of IVD degeneration (magnetic resonance imaging (MRI), histology, and immunohistochemistry (IHC)), and a total of 80 IVDs were randomly allocated for IVD degeneration analysis of the Intact control, Puncture (puncture only for preparation of degeneration), Discectomy (partial discectomy to create a cavity), Gel (partial discectomy and implantation of UPAL gel), and BMSCs + Gel (partial discectomy and implantation of BMSCs combined with UPAL gel) groups (8 IVDs per group). Four rabbits were used for analysis of viability of the implanted BMSCs using frozen sections of rabbit NP tissue; a total of 8 IVDs were randomly allocated to Intact control and BMSCs + Gel groups (4 IVDs per group). The remaining 12 rabbits were used for qualitative analysis of HIF-1α, GLUT-1, and Brachyury, which are proposed primary markers of healthy NPCs in humans [13], using IHC of paraffin sections of rabbit NP tissue as described

below; a total of 36 IVDs were randomly allocated to the Intact control, Discectomy, and BMSCs + Gel groups (4 IVDs per group).

2.7. BMSC labeling and encapsulation in UPAL solution

For *in vivo* experiments, we used OriCell^{TM} Rabbit Mesenchymal Stem Cells at passage 2 as the implanted cells as in the *in vitro* study. The BMSCs were labeled with CFDA-SE prior to implantation as described above and encapsulated in 2% UPAL solution, resulting in a final cell density of 1 $\times$ 10^6 cells/ml [14].

2.8. Induction of IVD degeneration and cell implantation

In this study, we used a rabbit annular puncture model to obtain degenerated IVDs as 20 week old rabbits are not sufficiently aged to mimic the condition in the aged human population and it is difficult to obtain older rabbits with uniform aging [8,15,16]. General anaesthesia was induced through intravenous injection of ketamine (10 mg/kg) and xylazine (3 mg/kg) and maintained with O_2 and air (3·0 l/min) mixed with sevoflurane (2−3%) in spontaneous ventilation. IVD degeneration was induced by AF puncture using an 18 gauge needle at the L2/3 and L4/5 IVDs (Supplementary Fig. 2). L3/4 IVDs were left intact as controls.

Four weeks after IVD puncture, UPAL solution containing BMSCs was implanted at the site of degenerated IVDs at L2/3 and L4/5 [8]. Under general anaesthesia, the spine was located via an antero-lateral retroperitoneal approach. In the Discectomy, Gel, and BMSCs + Gel groups, degenerated NP tissues were aspirated using 10 ml syringes and the remaining NP tissues removed using a micro ear forceps (Nagashima Medical Instruments Co. Ltd., Tokyo, Japan) at L2/3 and L4/5 IVDs (approximately 10−12 mg wet weight per IVD) to create an IVD cavity, after making a hole via 18-gauge needle puncture (Supplementary Fig. 3a). L3/4 IVDs were left intact as controls. In the Gel group, IVD defects were filled with 20 μl of 2% UPAL solution using a microsyringe (Hamilton Medical, Bonaduz, Switzerland) with a 27 gauge needle, and in the BMSCs + Gel group, IVD defects were filled with UPAL solution containing BMSCs. Notably, a 27 gauge needle was used because it has been shown that a 26 gauge needle did not affect cell viability or tissue degeneration [2,7,8,17]. Then, 1 ml of 102 mM $CaCl_2$ was injected on top of the UPAL solution to induce gelation (Supplementary Fig. 3b and c). After five min, the operative wound was washed with normal saline and closed. In the Puncture group, a sham procedure was performed. Rabbits were sacrificed by intravenous pentobarbital overdose at 4 and 12 weeks after surgery for analysis of IVD degeneration or at 1, 7, and 28 days after surgery for qualitative analysis of NPC markers. To evaluate the effects of human BMSCs on the rabbit IVDs, we also performed similar implantation experiments using human mesenchymal stem cells from bone marrow (hMSC-BM; PromoCell, Heidelberg, Germany; catalogue number: C-12974, lot number: 412Z022.4).

2.9. Detection of implanted BMSC viability

At 4 and 12 weeks after implantation, viability of the implanted BMSCs was qualitatively measured based on the CFDA-SE fluorescent label [18,19]. The IVDs (Intact control and BMSCs + Gel groups) were crosscut into halves, frozen in liquid nitrogen, sectioned into 5 μm slices, and then stained with 4′,6-diamidino-2-phenylindole (DAPI; Invitrogen; P36935) as a counterstain. Notably, it was not possible to quantify the viability of implanted BMSCs because DAPI-positive cells cannot be specified as viable *vs*. dead NPCs and BMSCs.

2.10. MRI analysis

At 4 and 12 weeks after surgery, T2-weighted midsagittal images of the IVDs were obtained using a 7·0-T MR scanner (Varian Unity

Inova; Varian Medical Systems, Palo Alto, CA, USA) [2,8,16]. The Pfirrmann classification scheme (grade 5 was classified as severely degenerated) was used to grade IVD degeneration [20]. Quantitative analysis was also performed to determine the MRI index using analyze software version 12.0 (AnalyzeDirect, Overland Park, KS, USA). The MRI index (the product of NP area and average signal intensity) was applied for the quantification of alterations in NP and quantitative data were expressed as a percentage relative to the MRI index obtained with untreated control IVDs (relative MRI index) [2,8,16].

2.11. Histological analysis

After MRI analysis, each IVD was processed for histological staining. Midsagittal sections (5 μm thick) were stained by haematoxylin and eosin (H&E) and safranin O-fast green for evaluation of proteoglycan expression [8]. Semiquantitative analyses of the IVDs were performed and graded from 0 (normal) to 5 (highly degenerative) [21,22]. Specifically, this histological scale focuses on the morphological changes in the AF structure.

2.12. IHC analysis

IHC staining was performed to detect type I and II collagen at 4 and 12 weeks after surgery [8], and HIF-1α, GLUT-1, and Brachyury at 1, 7, and 28 days after surgery. For type I and II collagen staining, mouse monoclonal antibodies against type I collagen (Sigma-Aldrich; C2456, RRID: AB_476836), and type II collagen (Kyowa Pharma Chemical, Toyama, Japan; F-57) were applied. Staining was developed using 3,3′-diaminobenzidine hydrochloride (Dako) and Mayer's haematoxylin (Merck, Darmstadt, Germany) as a counterstain. For HIF-1α, GLUT-1, and Brachyury staining, DyLight 550-conjugated rabbit polyclonal antibodies against HIF-1α (Novus Biologicals, Centennial, CO, USA; NB100-479R, RRID: AB_1642267), PE-conjugated rabbit polyclonal antibody against GLUT-1 (LS Bio, Seattle, WA, USA; LS-A109342-100), and unconjugated rabbit polyclonal antibodies against Brachyury (LS Bio; LS-C31179-100, RRID: AB_911118) were applied. Additionally, Alexa Fluor 594-conjugated goat anti-rabbit polyclonal antibodies (Invitrogen; A32740) were used as secondary antibodies for Brachyury. Staining was developed using DAPI as a counterstain.

Cells positive for type I and II collagen, HIF-1α, GLUT-1, and Brachyury were separately counted in five independent, randomly selected fields [2,8]. The fields spanned the width of the NP, including both deep and superficial regions. Values are expressed as the percentages of positive cells relative to total cell counts in all evaluation items and relative to CFDA-SE-positive cell counts for NPC marker evaluation. All experiments were performed on 8 IVDs for type I and II collagen evaluation and 4 IVDs for NPC marker evaluation from each treatment group and at each time point.

2.13. Statistical analysis

All data are presented as the means ± standard error (SE). One-way analysis of variance (ANOVA) and the Tukey−Kramer post hoc test were conducted for multigroup comparisons. Paired t-tests were performed for two-group comparisons. All statistical computations were carried out using JMP Pro-version 14.0 statistical software (SAS Institute, Cary, NC, USA) with a significance threshold of $p < 0.05$.

3. Results

3.1. NPC and BMSC co-culture promotes differentiation of BMSCs to NPCs and production of growth factors and ECM

To investigate the effects of NPC and BMSC co-culture on each cell type, unlabeled NPCs and CFDA-SE-labeled BMSCs were encapsulated in the UPAL gel for 3D cultures. In the co-culture group, we collected both cell types using a cell sorter. Phosphate buffered saline/cell suspension analysis was carried out using forward and side scatter. The P1 gate was drawn in a 2D dot plot (Fig. 1a) to exclude dead cells and debris. Unlabeled NPCs and CFDA-SE-labeled BMSCs were selected using different gates in the fluorescence *versus* side scatter dot plot (Fig. 1b). Therefore, the P2 gate was set over unlabeled cells and the P3 gate was set over CFDA-SE-labeled cells, leaving a gap between the two gates to avoid cross contamination [1]. Following gel dissolution and cell sorting, we obtained six types of cells as follows: (a) NPC control (at day0); (b) NPC mono-culture; (c) NPC co-culture; (d) BMSC control (at day0); (e) BMSC mono-culture; and (f) BMSC co-culture. For analysis of BMSC differentiation, we evaluated the gene expression of HIF-1, GLUT-1, and Brachyury as NPC markers, CDMP-1, TGF-β, and IGF-1 as growth factors, and type II collagen and aggrecan as ECM in the six types of cells using qRT-PCR.

The gene expression of HIF-1α in NPC co-culture was significantly increased compared with that in the NPC control ($p = 0.0218$, Tukey−Kramer test), and that in BMSC co-culture was significantly increased compared with those in the BMSC control ($p = 0.0041$, Tukey−Kramer test) and mono-culture ($p = 0.00116$, Tukey−Kramer test) (Fig. 1c). The expression of GLUT-1 in NPC co-culture showed a significant increase compared to that in the NPC control ($p < 0.0001$, Tukey−Kramer test) and mono-culture ($p < 0.0001$, Tukey−Kramer test), and that in NPC mono-culture showed a significant increase compared to expression in the NPC control ($p < 0.0001$, Tukey−Kramer test). BMSC co-culture showed a significant increase in GLUT-1 expression compared to that of the BMSC control ($p = 0.0189$, Tukey−Kramer test) (Fig. 1d). Conversely, the gene expression of Brachyury exhibited no statistical differences among the three types of NPC. Moreover, gene expression of Brachyury was only observed in the BMSC co-culture but not in either the BMSC control or mono-culture (Fig. 1e).

The gene expression of CDMP-1, TGF-β, and IGF-1 in NPC co-culture was significantly increased compared with that in NPC control ($p < 0.0001$, $p < 0.0001$, $p = 0.0002$, Tukey−Kramer test) and mono-culture ($p < 0.0001$, $p < 0.0001$, $p = 0.0082$, Tukey−Kramer test), expression in NPC mono-culture was significantly increased compared with that in the NPC control ($p = 0.0179$, $p < 0.0001$, $p = 0.0079$, Tukey−Kramer test), and expression in BMSC co-culture was significantly increased compared to that in the BMSC control ($p = 0.0011$, $p < 0.0001$, $p < 0.0001$, Tukey−Kramer test) and mono-culture ($p = 0.0015$, $p = 0.0386$, $p < 0.0001$, Tukey−Kramer test) (Fig. 1f–h).

The expression of type II collagen in NPC co-culture and mono-culture was significantly increased compared with that in the NPC control ($p = 0.0036$, $p = 0.0035$, Tukey−Kramer test), and that in BMSC co-culture was significantly increased compared with that in the BMSC control ($p = 0.004$, Tukey−Kramer test) and mono-culture ($p = 0.0226$, Tukey−Kramer test) (Fig. 1i). For aggrecan, the gene expression in NPC co-culture was significantly increased compared to that in the NPC control ($p = 0.0047$, Tukey−Kramer test) and mono-culture ($p = 0.0392$, Tukey−Kramer test), and expression in mono-culture was significantly increased compared to that in the NPC control ($p = 0.0274$, Tukey−Kramer test). Notably, aggrecan was only expressed upon BMSC co-culture but not in the BMSC control or mono-culture (Fig. 1j).

3.2. Viability of implanted BMSCs

In the *in vivo* study, CFDA-SE-labeled BMSCs were observed in the BMSCs + Gel groups but not in the Intact control groups at 4 and 12 weeks after surgery (Fig. 2). Human BMSC groups also showed similar findings as the BMSCs + Gel (rabbit BMSC) groups (Supplementary Fig. 4a), confirming that implanted BMSCs survived in the IVDs at 12 weeks after implantation. Upon dissection, no extrusion of the gel was noted.
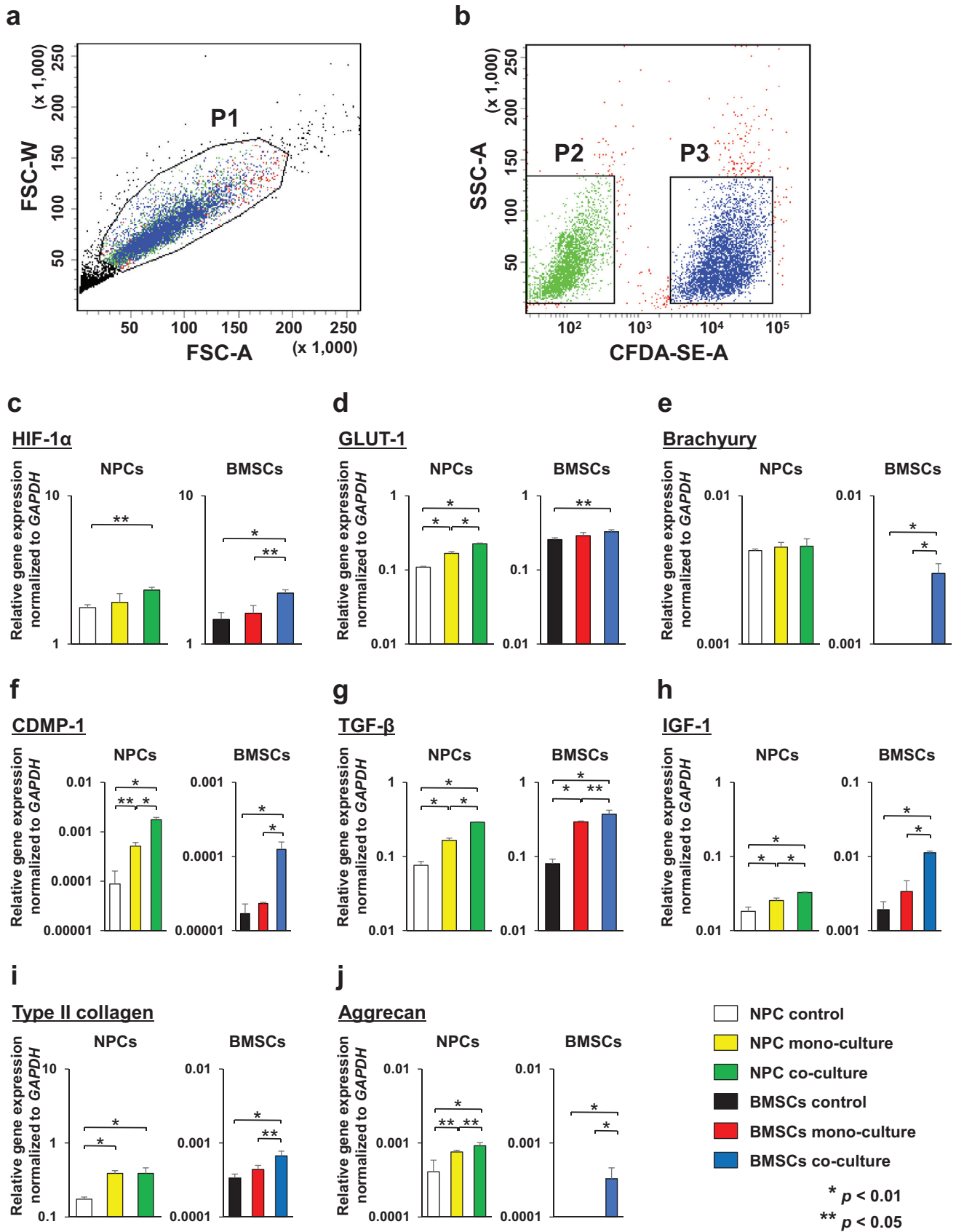
Fig. 1. Cell sorting data for separation of caboxyfluorescein diactetate succinimidyl ester (CFDA-SE)-labeled bone-derived mesenchymal stem cells (BMSCs) and unlabeled nucleus pulposus cells (NPCs) following 7-day co-culture using UPAL gel. (a): Two-dimensional (2D) dot plot for co-cultured cells. The P1 gate was placed around single live cells. (b): 2D dot plot showing unlabeled NPCs in the P2 gate and CFDA-SE-labeled BMSCs in the P3 gate that were sorted. FSC-A: Forward scatter-area; FSC-W: Forward scatter-width; SSC-A: Side scatter-area; CFDA-SE-A: CFDA-SE-area. Gene expression for each cell was normalized to the housekeeping gene *GAPDH* and plotted on a log scale (y-axis). Data were averaged from four different rabbit NPC lines. (c): HIF-1α, (d): GLUT-1, (e): Brachyury, (f): CDMP-1, (g): TGF-β, (h): IGF-1, (i): type II collagen, and (j): aggrecan. Data are represented as the means ± SE. *p*-values were determined by one-way ANOVA with a post hoc Tukey–Kramer test.
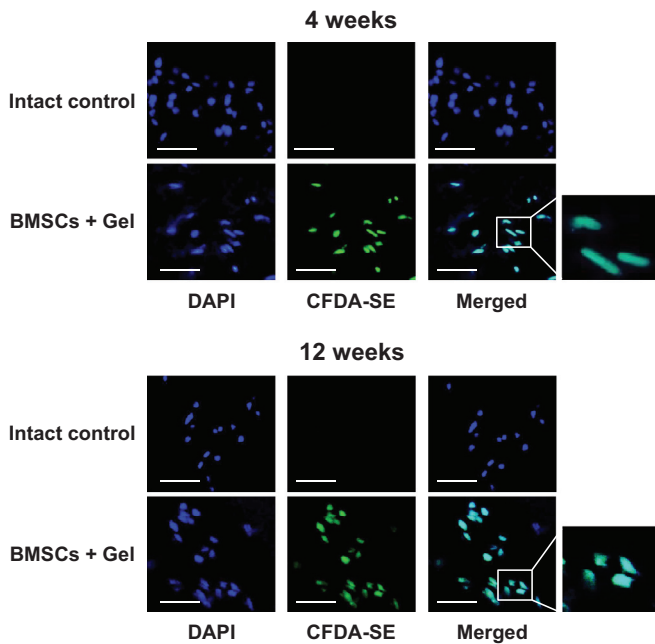
4 weeks

Intact control

BMSCs + Gel

DAPI   CFDA-SE   Merged

12 weeks

Intact control

BMSCs + Gel

DAPI   CFDA-SE   Merged

Fig. 2. Implanted bone-derived mesenchymal stem cells (BMSCs) labeled with caboxy-fluorescein diactetate succinimidyl ester (CFDA-SE) survive in intervertebral discs (IVDs) at 4 and 12 weeks after surgery. Frozen sections of IVD stained by 4′,6-diamino-2-phenylindole (DAPI). Images are representative of four replicates (Intact control and BMSCs + Gel, $n = 4$; 4 and 12 weeks). Scale bars = 50 μm.

3.3. Combination of BMSCs and UPAL gel promotes IVD regeneration following discectomy in degenerated IVDs

Degenerative changes in the treated IVDs were qualitatively analyzed by MRI, capturing T2-weighted, midsagittal images (Fig. 3a). The Pfirrmann grades in the BMSCs + Gel group were significantly lower than those in the Discectomy group at 4 weeks ($p = 0.003$, Tukey−Kramer test) and those in the Puncture and Discectomy groups at 12 weeks ($p = 0.0009$, $p < 0.0001$, Tukey−Kramer test). In addition, the grades in the Gel group were also significantly lower than those in the Discectomy group at 12 weeks ($p = 0.0028$, Tukey−Kramer test) (Fig. 3b). No significant difference was observed between the Gel and BMSCs + Gel groups. The MRI index in the BMSCs + Gel group was significantly higher than that in the Discectomy group at 4 weeks ($p = 0.0085$, Tukey−Kramer test) and those in the Puncture, Discectomy, and Gel groups at 12 weeks ($p = 0.0002$, $p < 0.0001$, $p = 0-0248$, Tukey−Kramer test). Additionally, the index in the Gel group was significantly higher than that in the Discectomy group at 12 weeks ($p = 0.0092$, Tukey−Kramer test) (Fig. 3c). Notably, no significant difference was observed between the rabbit BMSC and human BMSC groups in either the Pfirrmann grades or MRI index (Supplementary Fig. 4b−d).

Prior to the histological grading, the overall structures of IVDs including NP and AF were evaluated, with substantial differences observed among the groups. Histological evaluation of the IVDs revealed that intact control specimens exhibited typical, oval-shaped NP tissue, without structural collapse of the inner AF (Fig. 4a and b). In the Discectomy group, the inner had AF collapsed badly and fibrotic changes of NP tissue were observed at both 4 and 12 weeks. However, the inner AF in the BMSCs + Gel group appeared well preserved at both time points, with minimal fibrotic changes of NP tissue, and that in the Gel group also appeared relatively well-preserved (Fig. 4a and b). Accordingly, the scoring of degeneration as evaluated by histology in the BMSCs + Gel group was significantly lower than that in the Puncture ($p = 0.0006$, $p < 0.0001$, Tukey−Kramer test), Discectomy ($p < 0.0001$, $p < 0.0001$, Tukey−Kramer test), and Gel ($p = 0.00134$, $p < 0.0001$, Tukey−Kramer test) groups

at both 4 and 12 weeks, and that in the Gel group was significantly lower than that in the Discectomy group at 12 weeks ($p = 0.0006$, Tukey−Kramer test) (Fig. 4c). No significant difference was observed between the rabbit BMSC and human BMSC groups based on histological evaluation (Supplementary Fig. 5a and b). Osteophyte formation was not observed in any group.

3.4. Combination of BMSCs and UPAL gel promotes ECM production in degenerated IVDs

We next evaluated ECM production in IVDs. In particular, type II collagen constitutes an essential component necessary for IVD function whereas increase of type I collagen synthesis is observed in the IVD degeneration process [23]. The percentage of type II collagen-positive cells was significantly higher in the BMSCs + Gel group than those in the Puncture and Discectomy groups at 4 weeks ($p = 0.0001$, $p < 0.0001$, Tukey−Kramer test), and those in the Puncture, Discectomy, and Gel groups at 12 weeks ($p < 0.0001$, $p < 0.0001$, $p < 0.0001$, Tukey−Kramer test). In addition, the percentage in the Gel group was significantly higher than that in the Discectomy group at 4 weeks ($p < 0.0001$, Tukey−Kramer test), and those in the Puncture and Discectomy groups at 12 weeks ($p = 0.0231$, $p < 0.0001$, Tukey−Kramer test) (Fig. 5).

In contrast, the percentage of type I collagen-positive cells was significantly lower in the BMSCs + Gel group than those in the Puncture ($p < 0.0001$, $p < 0.0001$, Tukey−Kramer test), Discectomy ($p < 0.0001$, $p < 0.0001$, Tukey−Kramer test), and Gel ($p < 0.0001$, $p < 0.0001$, Tukey−Kramer test) groups at both 4 and 12 weeks. Moreover, the percentage was significantly lower in the Gel group than that in the Discectomy group at 4 weeks ($p < 0.0001$, Tukey−Kramer test) and in the Puncture and Discectomy groups at 12 weeks ($p = 0.0007$, $p < 0.0001$, Tukey−Kramer test) (Supplementary Fig. 6). No significant difference was observed between the rabbit BMSC and human BMSC groups based on IHC analysis (Supplementary Fig. 5c−f).

3.5. Implanted BMSC differentiation to NPCs in degenerated IVDs

Finally, we counted the HIF-1α, GLUT-1, and Brachyury-positive cells over time to consider the possible mechanism of implanted BMSC differentiation to NPCs *in vivo* (Fig. 6a−c). In the Intact control group, almost all cells were positive for the three NPC markers at all time points. In the BMSCs + Gel group, a low level of HIF-1α, GLUT-1, and Brachyury-positive cells was observed at day 1, whereas the number of positive cells increased over time. The percentages of the three types of NPC marker-positive cells relative to total cell counts were significantly higher at day 28 compared to those at days 1 and 7 ($p < 0.0001$, $p < 0.0001$, Student's t-test). Conversely, in the Discectomy group, around 20% of cells were positive at all time points (Fig. 6d−f). Similarly, the percentages of the three types of NPC marker-positive cells relative to CFDA-SE positive cell counts (representing implanted BMSCs) were significantly higher at day 28 compared to those at days 1 and 7 ($p < 0.0001$, $p < 0.0001$, Student's t-test) (Fig. 6g−i).

4. Discussion

Because the regenerative ability of IVDs is restricted, defects caused by discectomy may support insufficient tissue repair, leading to further IVD degeneration [2]. In the present study, whereas UPAL gel alone suppressed IVD degeneration compared to that following discectomy, the combination of BMSCs and UPAL gel exerted more potent effects to induce IVD regeneration. In addition, IVD regeneration was equally observed between human and rabbit BMSCs. Several previous studies have also demonstrated the regenerative ability of various BMSCs in degenerated IVDs [18,24,25]. Moreover, as UPAL
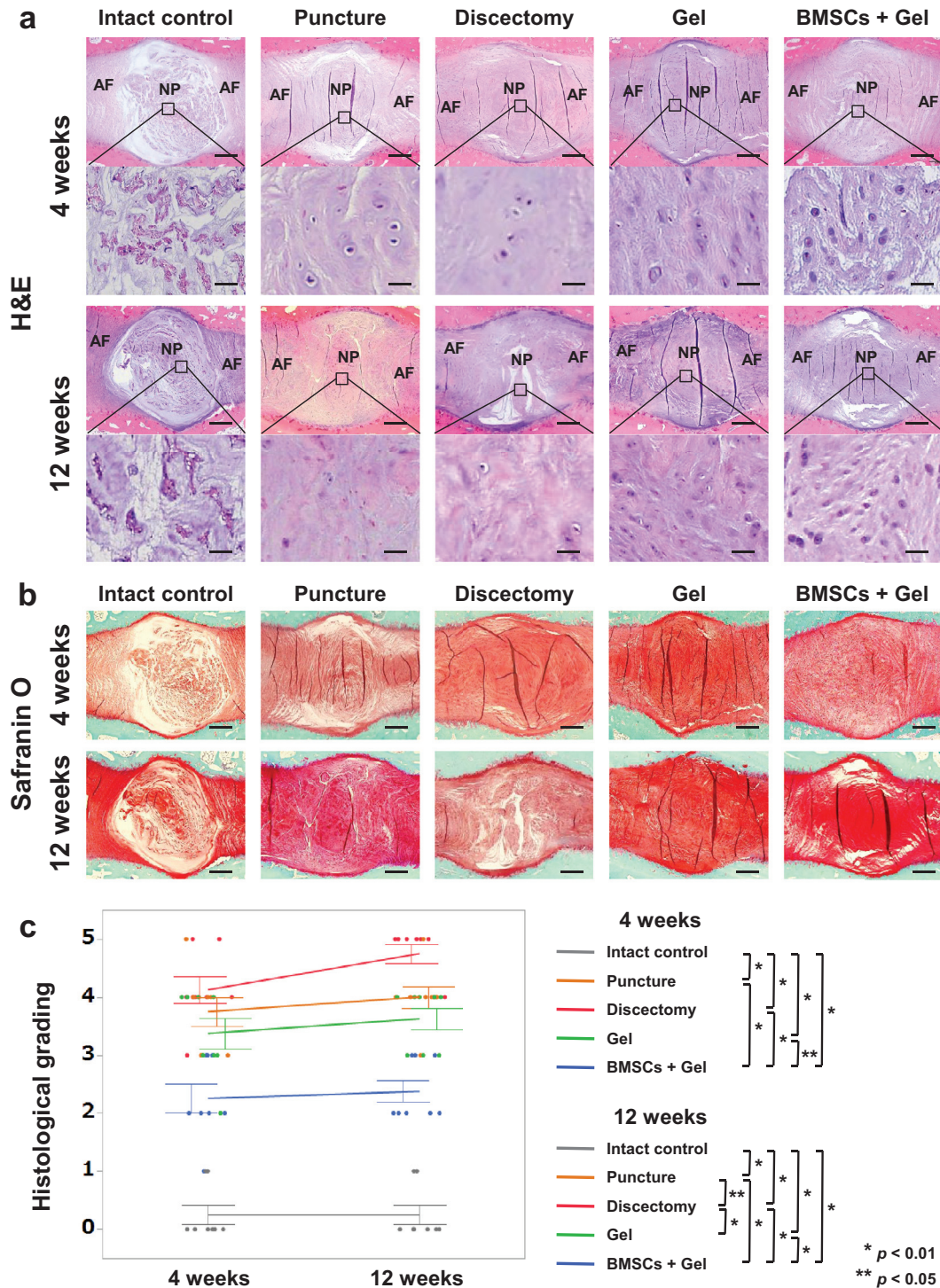
Fig. 3. Gel combined with bone-derived mesenchymal stem cells (BMSCs) preserve the water content of degenerated intervertebral discs (IVDs) following discectomy. (a): T2-weighted, midsagittal images of degenerated IVDs at 4 and 12 weeks after surgery. Images are representative of eight replicates. (b): Pfirrmann grading of IVD degeneration. Data are the means ± SE (Intact control, Puncture, Discectomy, Gel, and BMSCs + Gel, n = 8; 4 and 12 weeks). (c) Magnetic resonance imagining (MRI) index (nucleus pulposus (NP) area × average signal intensity) for degenerative alterations of the NP. Numerical values are expressed as percentages, compared with intact control IVDs. Data are the means ± SE. p-values were determined by one-way ANOVA with post hoc analysis using the Tukey−Kramer test.

gel exhibits high biocompatibility and sufficient biomechanical characteristics to support an endogenous reparative therapeutic strategy [2], it provides an optimal environment for IVD regeneration and the prevention of further degeneration following BMSC implantation at the site of degenerative IVDs.

In the current study, the gene expression of NPC markers, growth factors, and ECM was significantly increased in NPC and BMSC 3D co-culture compared to each 3D mono-culture *in vitro*. Various cells express HIF-1α and GLUT-1. In this study, although the NPC control did not express higher levels of NPC markers than those of the BMSC controls, these markers were significantly increased in the co-culture. These results suggested that BMSC co-culture with NPCs led to BMSC differentiation into NPCs, which in turn led to a mutual activation effect between NPCs and BMSCs, resulting in enhancement of ECM production in both cell types. This is consistent with the findings of several other *in vitro* studies that have also shown that co-culture of

Fig. 4. Gel combined with bone-derived mesenchymal stem cells (BMSCs) prevents intervertebral disc (IVD) degeneration following discectomy. (a, b): Midsagittal sections of IVDs stained by haematoxylin and eosin (H&E) or safranin O. Images are representative of eight replicates (Intact control, Puncture, Discectomy, Gel, BMSCs + Gel, n = 8; 4 and 12 weeks). AF; annulus fibrosus, NP; nucleus pulposus. Scale bars = (A): 500 μm (first and third sections from the top), 50 μm (second and fourth sections from the top) and (B): 500 μm. (c): Histological grading at 4 and 12 weeks is shown. Data are the means ± SE. p-values were determined by one-way ANOVA with the post hoc Tukey−Kramer test.

NPCs and BMSCs stimulates BMSCs to differentiate into an NPC-like phenotype [1,12,26], supporting interactive activation between NPCs and BMSCs through the production of growth factors [1,11,27] and up-regulation of ECM synthesis [1,5,10,26].

Additionally, similar results were observed in the *in vivo* study showing increased expression of NPC markers in implanted BMSCs over time, and enhanced ECM production compared to the results following discectomy alone. Although to our knowledge no reports have

considered the possible mechanism of implanted BMSC differentiation to NPCs *in vivo* using alginate and BMSCs, one study documented that implanted MSCs embedded in atelocollagen could differentiate into NPCs [28]. Specifically, autologous BMSCs labeled with green fluorescent protein were transplanted into mature rabbit IVDs and the differentiation of transplanted cells was determined by IHC analysis. At 48 weeks after transplantation, implanted BMSCs were shown to be positive for HIF-1α, GLUT-1, and MMP-2, indicating that
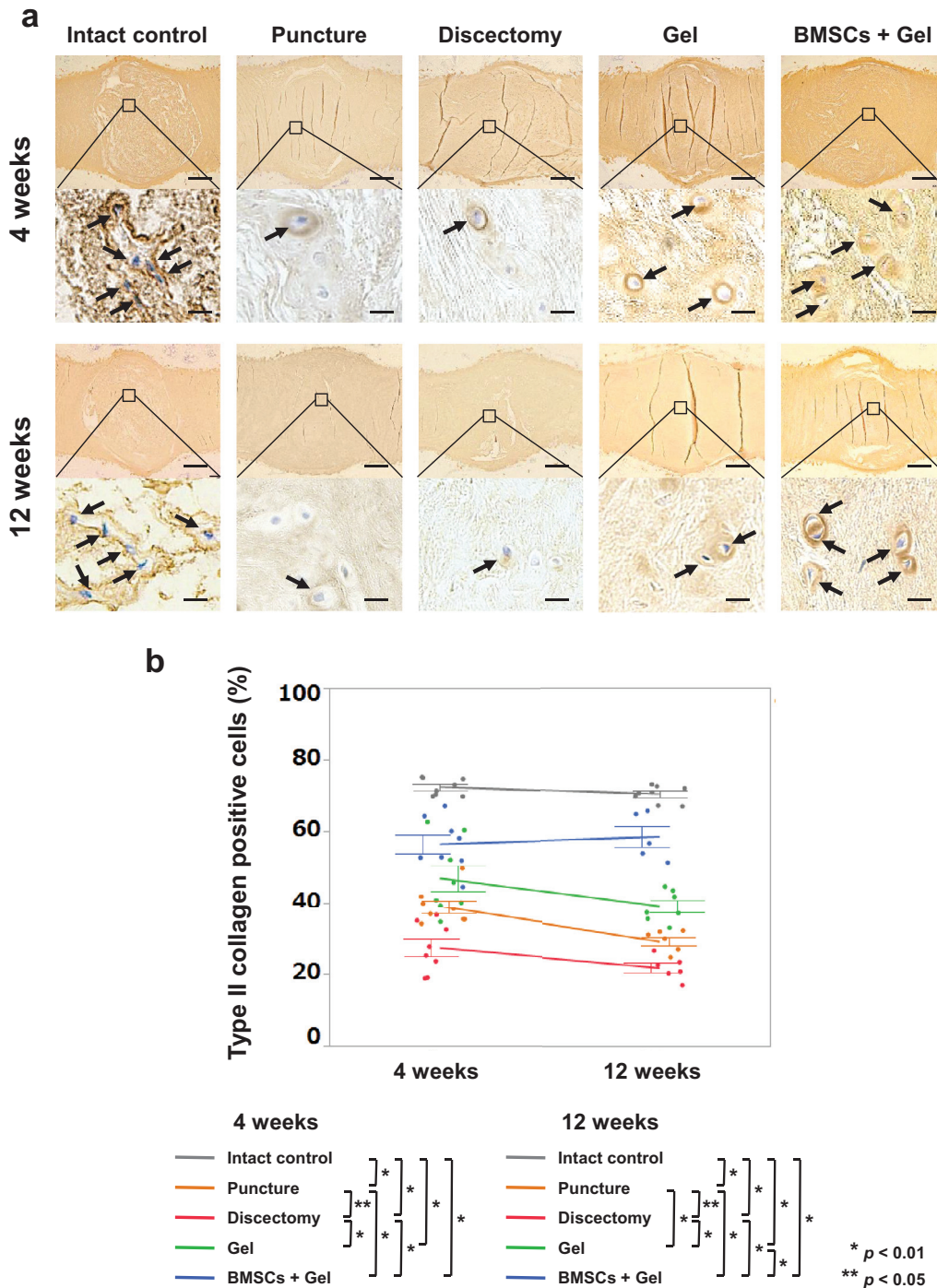
Fig. 5. Type II collagen-positive cells in rabbit nucleus pulposus (NP). (a): Midsagittal sections of rabbit intervertebral discs (IVDs) stained for type II collagen. Images are representative of eight replicates (Intact control, Puncture, Discectomy, Gel, BMSCs + Gel, $n = 8$; 4 and 12 weeks). Arrows indicate cells positive for type II collagen. Scale bars = 500 μm (first and third sections from the top) and 20 μm (second and fourth sections from the top). (b): Percentages of type II collagen-positive cells. Data are the means ± SE. p-values were determined by one-way ANOVA with the post hoc Tukey−Kramer test.

BMSCs differentiated into cells expressing some of the representative phenotypic features of NPCs [28].

In the *in vivo* study, histological analysis further suggested that implantation of gel alone prevents IVD degeneration compared to that following discectomy, and that the combination of BMSCs + Gel exhibits more potent effects on prevention of degeneration. This is consistent with the MRI findings, which suggested that gel alone preserves the water content of IVDs compared to discectomy, whereas the BMSCs + Gel combination yields more potent effects on water content preservation. IHC results further suggested that the BMSCs + Gel

combination promotes ECM synthesis in degenerated NP tissue, which is crucial to proper IVD function and led to the prevention of progressive degeneration through the depressed production of type I collagen. Furthermore, the histological results of BMSCs + Gel compared to those of the Puncture group (degenerated IVDs without discectomy) suggested that BMSC implantation led to IVD regeneration. Together, these results suggested that implanted BMSCs differentiate to NPCs over time, resulting in IVD regeneration *in vivo*.

With regard to AF regeneration, although the Gel and BMSCs + Gel groups exhibited significantly decreased collagen I production in the
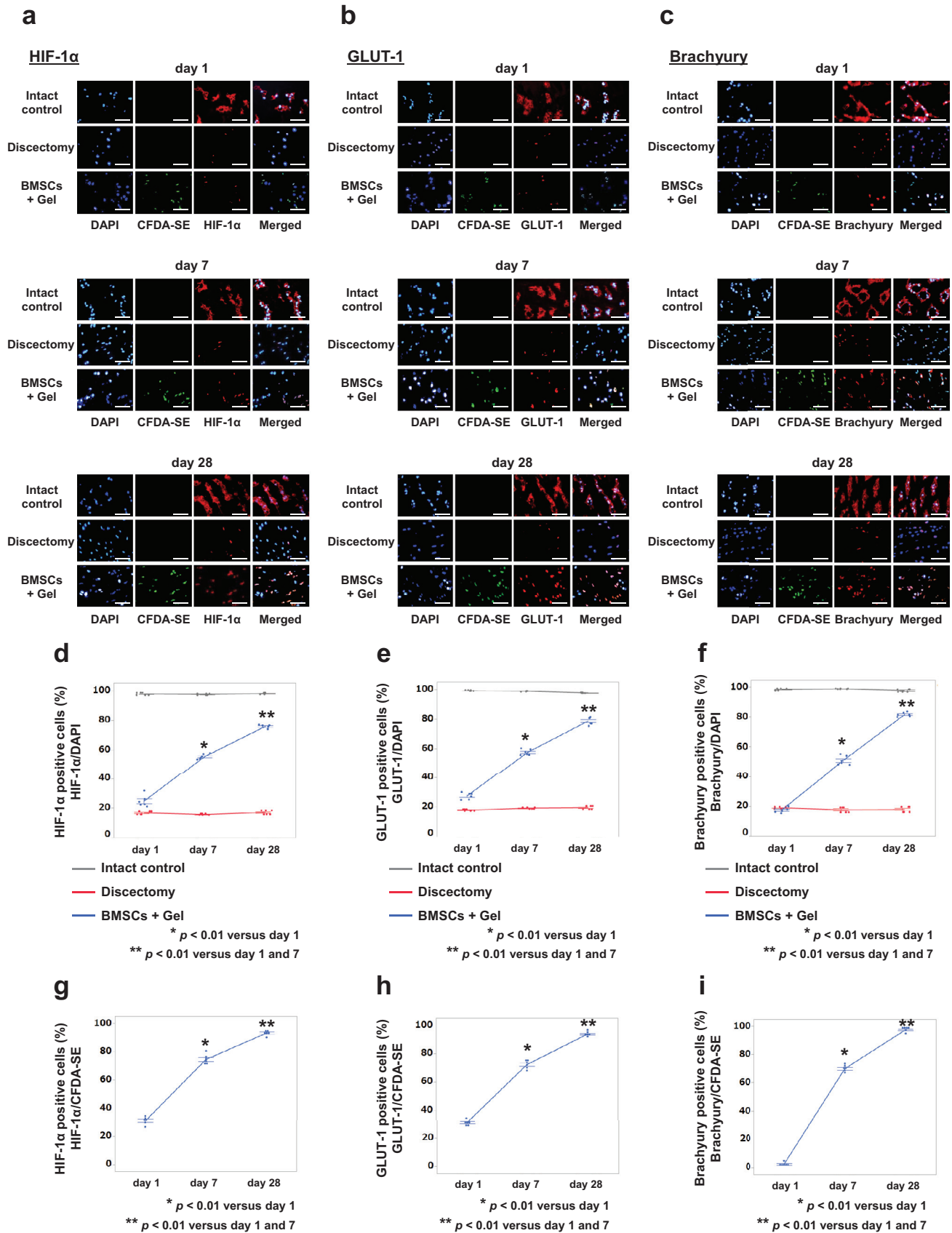
Fig. 6. Nucleus pulposus (NP) marker-positive cells in rabbit NPs. (a–c): Horizontal sections of rabbit intervertebral discs (IVDs) stained for HIF-1α, GLUT-1, and Brachyury at days 1, 7, and 28. Images are representative of four replicates (Intact control, Discectomy, and BMSCs + Gel, $n = 4$; days 1, 7, and 28). Scale bar = 50 μm. (d–f): Percentages of NP marker-positive cells relative to total cells. (g–i): Percentages of NP marker-positive cells relative to CFDA-SE-positive cells (representative of implanted BMSCs). Data are the means ± SE. p-values were determined using the paired t-test.

NP, the punctured AF defect was repaired. Because IVD degeneration is marked by degradation of the NP extracellular matrix [2], the present study focused principally on the preservation/regeneration of the NP. In addition, morphological changes in the AF structure were evaluated using a histological scale; nevertheless, detailed evaluation of AF regeneration is warranted in future studies.

Notably, some studies have reported the risk of BMSC leakage from the injection site, resulting in osteophyte formation [5,29,30]. Therefore, carrier materials are required for prevention of cell leakage in the case of BMSC implantation following discectomy. In our study, osteophyte formation was not observed in the BMSCs + Gel group. Owing to the crucial characteristic of rapid curing, the combination use of UPAL gel with BMSCs thus offers another clinical advantage in terms of preventing cell leakage.

Based on the results of the present study and previous reports [1,11,12,26−28], we therefore considered that the possible mechanism of IVD regeneration is as follows. 1) Implanted BMSCs can localize in the cavity of IVDs without leakage through encapsulation in the UPAL gel. 2) Implanted BMSCs produce growth factors and ECM, resulting in activation of the existing NPCs. 3) Activated NPCs also increase the production of growth factors and ECM. 4) Consequently, implanted BMSCs differentiate into NPCs. 5) In addition, BMSCs and existing NPCs activate each other, resulting in IVD regeneration (Fig. 7). We consider that cell−cell interaction is unlikely to constitute the main mechanism of action of IVD degeneration because few distinct cell types would be present if the majority of BMSCs and NPCs were fused as in the current in vitro experiments. Moreover, BMSCs and NPCs did not directly contact each other in vivo. Accordingly, the underlying mechanism of action may be due to growth factors and/or some critical secreted factors that regulate the crosstalk between BMSCs and NPCs.

In the present study, the use of commercially available BMSCs represents an apparent strength, as presumably the cell source affords quality MSCs with minimal batch-to-batch variability. Moreover, although the BMSCs were not characterised according to the International Society for Cellular Therapy (ISCT) criteria [31] and no ISCT criteria yet exist for rabbit BMSCs, characterization of the human BMSCs used in the present study according to the ISCT criteria has previously been published [32].

This study has a few limitations. First, the animal models of IVD degeneration implemented in the present study were generated using rabbit IVDs and therefore do not strictly imitate the surgical procedure of discectomy executed clinically. Further experimental studies using a large animal model might address whether BMSCs combined with UPAL gel is useful for lumbar discectomy. Second, radiographic assays were not conducted to precisely measure IVD height. Rather, we attempted to measure the height of the IVD using MRI images. However, in the degenerated IVDs, accurate measurements were not feasible because the borders between IVDs and vertebrae were unclear. Third, only a single BMSC concentration was utilised. Although a concentration-response curve would have been relevant to establish the most effective cell concentration, the MSC concentration utilised in our study (1×10^6 cells/ml) was based in large part on the results of a previous study conducted in vivo using a canine IVD degeneration model to determine optimal MSC number [33]. Specifically, autologous MSCs were transplanted into degenerative discs at 1×10^5, 1×10^6, or 1×10^7 cells per disc; the results showed that both the structural microenvironment and abundant extracellular matrix were maintained using 1×10^6 transplanted IVDs compared to 1×10^5 or 1×10^7 transplanted IVDs [33]. We therefore selected 1×10^6 cells/ml based on these results and those on another study [14]. Fourth, although the expression of HIF-1α, GLUT-1, and Brachyury was increased in the co-culture group, the increase was marginal. In this study, we were unable to perform western blot analysis or enzyme-linked immunosorbent assay to double confirm these results or those for CDMP-1, TGF-β, and IGF-1 because the appropriate anti-rabbit antibodies were not available.

5. Conclusions

Discectomy to treat degenerated IVD may offer temporary relief but may not induce tissue repair, especially in elderly patients with fewer endogenous NPCs, and does not address the potential for further degeneration. In the present study we demonstrated that the combination of BMSCs with UPAL gel in vitro, and transplantation thereof in vivo following partial discectomy in a rabbit model, promoted endogenous NPC activation together with BMSCs activation and differentiation into NPCs, together with growth factor and ECM production and enhanced IVD regeneration. Notably, similar results were obtained with either rabbit or human BMSCs. Thus, these findings demonstrate the additional therapeutic potential of BMSCs, localized at the IVD site by UPAL gel, as a regenerative strategy following discectomy for degenerated IVDs and support the future evaluation of this approach in a clinical setting, especially in an older population cohort.
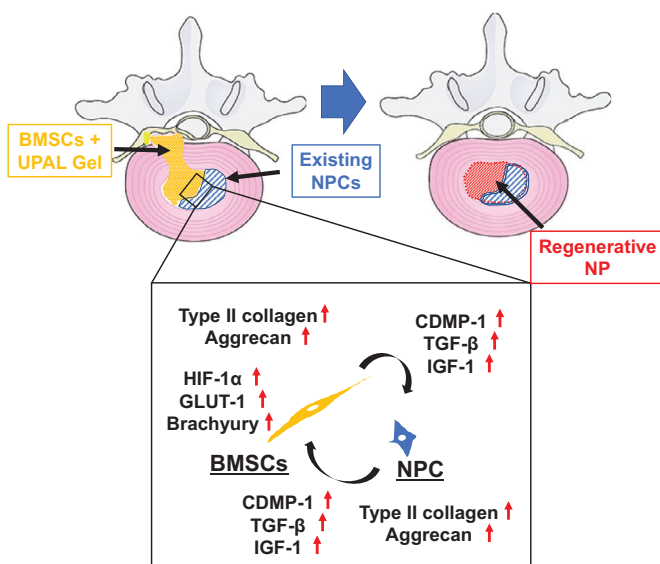
Fig. 7. Possible mechanism of intervertebral disc (IVD) regeneration. Implanted bone-derived mesenchymal stem cells (BMSCs) produce growth factors and extracellular matrix (ECM) resulting in activation of the existing nucleus pulposus cells (NPCs). Existing NPC activation also increases the production of growth factors and ECM. Implanted BMSCs differentiate into NPCs. UPAL, ultra-purified alginate.

Author Contributions

H.S. conceived and designed the study. D.U., H.S., T.T., and K.U. performed the experiments. D.U. and H.S. analyzed the results. D.U., H.S., K.Y., and N.I. contributed to discussions throughout the study. D. U. and H.S. wrote and edited the manuscript. All authors had full access to all data of this study and had final responsibility for the decision to submit for publication.

Supplementary materials

Supplementary material associated with this article can be found in the online version at doi:10.1016/j.ebiom.2020.102698.

References

[1] Strassburg S, Richardson SM, Freemont AJ, Hoyland JA. Co-culture induces mesenchymal stem cell differentiation and modulation of the degenerate human nucleus pulposus cell phenotype. Regen Med 2010;5(5):701–11.

[2] Tsujimoto T, Sudo H, Todoh M, et al. An acellular bioresorbable ultra-purified alginate gel promotes intervertebral disc repair: a preclinical proof-of-concept study. EBioMedicine 2018;37:521–34.

[3] Oehme D, Ghosh P, Shimmon S, et al. Mesenchymal progenitor cells combined with pentosan polysulfate mediating disc regeneration at the time of microdiscectomy: a preliminary study in an ovine model. J Neurosurg Spine 2014;20(6):657–69.

[4] Noriega DC, Ardura F, Hernández-Ramajo R, et al. Intervertebral disc repair by allogeneic mesenchymal bone marrow cells: a randomized controlled trial. Transplantation 2017;101(8):1945–51.

[5] Naqvi SM, Buckley CT. Differential response of encapsulated nucleus pulposus and bone marrow stem cells in isolation and coculture in alginate and chitosan hydrogels. Tissue Eng Part A 2015;21(1−2):288–99.

[6] Sudo H.Exploratory clinical trial on the safety and capability of dMD-001 in lumbar disc herniation. https://upload.umin.ac.jp/cgi-open-bin/icdr_e/ctr_view.cgi?recptno=R000039018. Accessed December 10, 2019.

[7] Yamada K, Sudo H, Iwasaki K, et al. Caspase 3 silencing inhibits biomechanical overload-induced intervertebral disk degeneration. Am J Pathol 2014;184 (3):753–64.

[8] Sudo H, Minami A. Caspase 3 as a therapeutic target for regulation of intervertebral disc degeneration in rabbits. Arthritis Rheum 2011;63(6):1648–57.

[9] Sato M, Uchida K, Nakajima H, et al. Direct transplantation of mesenchymal stem cells into the knee joints of Hartley strain guinea pigs with spontaneous osteoarthritis. Arthritis Res Ther 2012;14(1):R31.

[10] Ouyang A, Cerchiari AE, Tang X, et al. Effects of cell type and configuration on anabolic and catabolic activity in 3D co-culture of mesenchymal stem cells and nucleus pulposus cells. J Orthop Res 2017;35(1):61–73.

[11] Yamamoto Y, Mochida J, Sakai D, et al. Upregulation of the viability of nucleus pulposus cells by bone marrow-derived stromal cells: significance of direct cell-to-cell contact in coculture system. Spine (Phila Pa 1976) 2004;29(14):1508–14.

[12] Richardson SM, Walker RV, Parker S, et al. Intervertebral disc cell-mediated mesenchymal stem cell differentiation. Stem Cells 2006;24(3):707–16.

[13] Risbud MV, Schoepflin ZR, Mwale F, et al. Defining the phenotype of young healthy nucleus pulposus cells: recommendations of the Spine Research Interest Group at the 2014 annual ORS meeting. J Orthop Res 2015;33(3):283–93.

[14] Hiyama A, Mochida J, Iwashina T, et al. Transplantation of mesenchymal stem cells in a canine disc degeneration model. J Orthop Res 2008;26(5):589–600.

[15] Lei T, Zhang Y, Zhou Q, et al. A novel approach for the annulus needle puncture model of intervertebral disc degeneration in rabbits. Am J Transl Res 2017;9 (3):900–9.

[16] Ura K, Sudo H, Iwasaki K, Tsujimoto T, Ukeba D, Iwasaki N. Effects of intradiscal injection of local anesthetics on intervertebral disc degeneration in rabbit degenerated intervertebral disc. J Orthop Res 2019;37(9):1963–71.

[17] Qian J, Ge J, Yan Q, Wu C, Yang H, Zou J. Selection of the optimal puncture needle for induction of a rat intervertebral disc degeneration model. Pain Physician 2019;22(4):353–60.

[18] Wang H, Zhou Y, Huang B, et al. Utilization of stem cells in alginate for nucleus pulposus tissue engineering. Tissue Eng Part A 2014;20(5−6):908–20.

[19] Polzer H, Volkmer E, Saller MM, et al. Long-term detection of fluorescently labeled human mesenchymal stem cell in vitro and in vivo by semi-automated microscopy. Tissue Eng Part C Methods 2012;18(2):156–65.

[20] Pfirrmann CW, Metzdorf A, Zanetti M, Hodler J, Boos N. Magnetic resonance classification of lumbar intervertebral disc degeneration. Spine (Phila Pa 1976) 2001;26(17):1873–8.

[21] Sakai D, Mochida J, Iwashina T, et al. Regenerative effects of transplanting mesenchymal stem cells embedded in atelocollagen to the degenerated intervertebral disc. Biomaterials 2006;27(3):335–45.

[22] Nishimura K, Mochida J. Percutaneous reinsertion of the nucleus pulposus: an experimental study. Spine (Phila Pa 1976) 1998;23(14):1531–8.

[23] Le Maitre CL, Pockert A, Buttle DJ, Freemont AJ, Hoyland JA. Matrix synthesis and degradation in human intervertebral disc degeneration. Biochem Soc Trans 2007;35(Pt 4):652–5.

[24] Wang F, Nan LP, Zhou SF, et al. Injectable hydrogel combined with nucleus pulposus-derived mesenchymal stem cells for the treatment of degenerative intervertebral disc in rats. Stem Cells Int 2019:8496025.

[25] Omlor GW, Lorenz S, Nerlich AG, Guehring T, Richter W. Disc cell therapy with bone-marrow-derived autologous mesenchymal stromal cells in a large porcine disc degeneration model. Eur Spine J 2018;27(10):2639–49.

[26] Risbud MV, Albert TJ, Guttapalli A, et al. Differentiation of mesenchymal stem cells towards a nucleus pulposus-like phenotype in vitro: implications for cell-based transplantation therapy. Spine (Phila Pa 1976) 2004;29(23):2627–32.

[27] Yang SH, Wu CC, Shih TT, Sun YH, Lin FH. In vitro study on interaction between human nucleus pulposus cells and mesenchymal stem cells through paracrine stimulation. Spine (Phila Pa 1976) 2008;33(18):1951–7.

[28] Sakai D, Mochida J, Iwashina T, et al. Differentiation of mesenchymal stem cells transplanted to a rabbit degenerative disc model: potential and limitations for stem cell therapy in disc regeneration. Spine (Phila Pa 1976) 2005;30(21):2379–87.

[29] Li YY, Diao HJ, Chik TK, et al. Delivering mesenchymal stem cells in collagen microsphere carriers to rabbit degenerative disc: reduced risk of osteophyte formation. Tissue Eng Part A 2014;20(9−10):1379–91.

[30] Vadalà G, Sowa G, Hubert M, Gilbertson LG, Denaro V, Kang JD. Mesenchymal stem cells injection in degenerated intervertebral disc: cell leakage may induce osteophyte formation. J Tissue Eng Regen Med 2012;6(5):348–55.

[31] Dominici M, Le Blanc K, Mueller I, et al. Minimal criteria for defining multipotent mesenchymal stromal cells. The International Society for Cellular Therapy position statement. Cytotherapy 2006;8(4):315–7.

[32] Raynaud CM, Maleki M, Lis R, et al. Comprehensive characterization of mesenchymal stem cells from human placenta and fetal membrane and their response to osteoactivin stimulation. Stem Cells Int 2012;2012:658356.

[33] Serigano K, Sakai D, Hiyama A, Tamura F, Tanaka M, Mochida J. Effect of cell number on mesenchymal stem cell transplantation in a canine disc degeneration model. J Orthop Res 2010;28:1267–75.